Heinrich Heine
Universität
Düsseldorf

Serum-free differentiation platform for the generation of B lymphocytes and natural killer cells from human CD34+ cord blood progenitors

Rigveda Bhave, Carla-Johanna Kath, Nadine Rüchel, Eleni Vasileiou, Vera H. Jepsen, Katharina Raba, Aleksandra A. Pandyra, Ute Fischer & Gesine Kogler

Article - Version of Record

Suggested Citation:
Bhave, R. N., Kath, C.-J., Rüchel, N., Vasileiou, E., Jepsen, V., Raba, K., Pandyra, A. A., Fischer, U., & Kögler, G. (2025). Serum-free differentiation platform for the generation of B lymphocytes and natural killer cells from human CD34+ cord blood progenitors. Scientific Reports, 15, Article 44132. https://doi.org/10.1038/s41598-025-30732-9

Wissen, wo das Wissen ist.

UNIVERSITÄTS- UND LANDESBIBLIOTHEK DÜSSELDORF

This version is available at:

URN: https://nbn-resolving.org/urn:nbn:de:hbz:061-20260123-125348-3

Terms of Use:

This work is licensed under the Creative Commons Attribution 4.0 International License.

For more information see: https://creativecommons.org/licenses/by/4.0

scientific reports

Check for updates

OPEN

Serum-free differentiation platform for the generation of B lymphocytes and natural killer cells from human CD34+ cord blood progenitors

Rigveda Bhave[1,2,3,4]✉, Carla-Johanna Kath[1,2,3], Nadine Rüchel[2,3,4], Eleni Vasileiou[2,4,5,6], Vera H. Jepsen[2,3,4], Katharina Raba[1], Aleksandra A. Pandyra[2,4,5,6], Ute Fischer[2,3,4] & Gesine Kogler[1]

Pre-clinical research on B and NK cell development relies on murine stromal cell-based systems with reduced physiological relevance and clinical applicability. A serum-free, fully humanized co-culture system utilizing human bone marrow-derived mesenchymal stromal cells (BM-MSCs) was developed to differentiate CB-CD34+ cells towards B and NK cell lineages. Differentiation dynamics were monitored via flow cytometry, with immunophenotypic analysis tracking progression from progenitors to mature cells. The system generated CD19+ IgM+ immature B cells and CD56+ CD16+ NK cells, recapitulating fetal stages of human lymphopoiesis. Serum-free media conditions ensured reproducibility and high overall yield of CD19+ B (35 ± 5.32%) and CD56+ NK (28.46 ± 7.01%) cell progenitors. Flow cytometry identified distinct population peaks, confirming temporal control over differentiation. This clinically relevant platform addresses the limitations of traditional models by providing a more physiologically accurate human microenvironment. The serum-free system supports applications in disease modeling, genotoxic compound screening, and mutational studies of hematopoiesis. By enabling scalable production of B and NK cells it aims to accelerate translational research for immunodeficiencies, cancer immunotherapy, and hematopoietic disorders.

Keywords Cord blood, B lymphocytes, Culture media, Serum-free, Cell differentiation, Killer cells, Natural, Mesenchymal stem cells

Hematopoietic stem and progenitor cells (HSPCs) derived from umbilical cord blood (CB) harbour the potential to self-renew and give rise to all mature blood lineages[1–3]. CB HSPCs are an established source of transplant material for the treatment of hematologic malignancies, bone marrow failure syndromes, hemoglobinopathies and immune deficiencies, where they restore the entire hematopoietic hierarchy in the recipient[4–6]. Several therapies are under development using cells differentiated from CB HSPCs including native/chimeric antigen receptor (CAR) natural killer (NK) cells and CAR T cell therapies[7–9]. Despite these advances, basic translational research frequently utilizes traditional cell culture systems using immortalized murine stromal cells as a supportive microenvironment[10]. These are not conducive to therapeutic/clinical downstream applications and have lower physiological relevance. Moreover, the investigation of B cell and NK cell development is limited by the absence of model systems capable of accurately recapitulating human fetal hematopoiesis under laboratory conditions.

[1]Institute for Transplantation Diagnostics and Cell Therapeutics, Medical Faculty and University Hospital Düsseldorf, Heinrich Heine University, Düsseldorf, Germany. [2]Department of Pediatric Oncology, Hematology and Clinical Immunology, Medical Faculty and University Hospital Düsseldorf, Heinrich Heine University, Düsseldorf, Germany. [3]German Cancer Consortium (DKTK), Partner Site Essen/Düsseldorf, Düsseldorf, Germany. [4]Center for Integrated Oncology Aachen Bonn Cologne Düsseldorf (CIO ABCD), Bonn, Germany. [5]Institute of Clinical Chemistry and Clinical Pharmacology, University Hospital Bonn, Bonn, Germany. [6]German Center for Infection Research (DZIF), Partner Site Bonn-Cologne, Bonn, Germany. ✉email: RigvedaNitin.Bhave@med.uni-duesseldorf.de

Because B cell precursors of fetal or adult origin are difficult to source in sufficient quantities, the demand for in vitro model systems for efficient expansion and differentiation is high. From the earliest CD34+ hematopoietic progenitors to immunophenotypically characterized lineage-restricted cells, the developmental potential towards the B lineage commitment has frequently been evaluated in co-culture systems using the MS-5 murine stromal cell line[11–14]. Previous studies have highlighted the drawbacks of utilizing stromal cells of murine origin, showing that human bone marrow-derived mesenchymal stromal cells (BM-MSCs) have a greater capacity to promote B cell lymphopoiesis[15–17]. While there are multiple high-quality protocols for generating NK cells for clinical applications, these require complex media preparations and often utilize proprietary feeder cell lines and/or specialized coatings[18–20].

This article presents a novel, user-friendly, serum-free co-culture system for the differentiation of CB-derived CD34+ HSPCs into either CD19+ IgM+ immature B cells or CD56+ NK cells, contingent upon the cytokine cocktail employed. The differentiation process is monitored by flow cytometry, enabling precise identification of the time points at which distinct cell populations peak. Immunophenotypic analysis using progenitor-specific markers confirms that this model recapitulates B and NK cell lineage hematopoiesis up to the IgM+ immature B cell and CD56+ CD16+ NK cell stages, respectively. In contrast to previously established laboratory-scale models, this approach utilizes a fully humanized system, co-culturing CD34+ CD45low HSPCs isolated from cord blood with a human bone marrow-derived mesenchymal stromal cell (BM-MSC) line[21] and recombinant human cytokines. The serum-free conditions support robust generation of B and NK cell lineage progenitors, facilitating applications in disease modeling, therapeutic and genotoxic compound testing, and mutational studies affecting hematopoietic development.

Results

CB CD34+ HSPCs expand in B differentiation conditions and generate lymphoid-primed progenitors

There is substantial variability in the percentage of CD34+ cells among different CB units, influenced by factors such as gestational age, birth conditions and inherent biological heterogeneity[22–24]. CD34+CD45low cells were isolated from n = 9 biologically distinct CB units. Given the importance of generating sufficient differentiated hematopoietic cells from a limited CD34+ cell input, hematopoietic cell proliferation was monitored throughout the B cell differentiation culture period. Since hematopoietic cells only loosely adhere to the BM-MSC feeder layer, manual cell counts were conducted by gently resuspending the cells in the well without disturbing the feeder layer. During later time points, detachment of non-viable feeder cells was observed; however, these cells could be excluded from the count based on their larger size and positive Trypan blue staining. By day 35, a cumulative population doubling of 44.69 ± 0.90 was observed in hematopoietic cell numbers, indicating robust generation of progenitors (Fig. 1A).

There were significant differences between the yields and composition of CD34+CD45low HSPCs isolated on day 0 (Fig. 1B). Immunophenotypic characterization of the HSPC progenitor populations on day 0 showed that the majority of CD34+ cells isolated from CB were MPPs (CD34+CD38-CD90-) (21.68 ± 10.23%), CMPs (CD34+CD38+CD135+) (19.62 ± 7.92%) and GMPs (CD34+CD38+CD135+CD45RA+) (24.08 ± 10.44%) (Fig. 1B). Overall, CB samples exhibited a myeloid progenitor (CMP, GMP, MEP) composition between 45 and 60%. After day 21, the fraction of CD34+ cells that were not already lineage committed (CD34+LIN+) was negligible, and therefore not analyzed (Fig. 1C). The gating strategy for HSPC characterization was performed as shown (Supplementary Fig. 1).

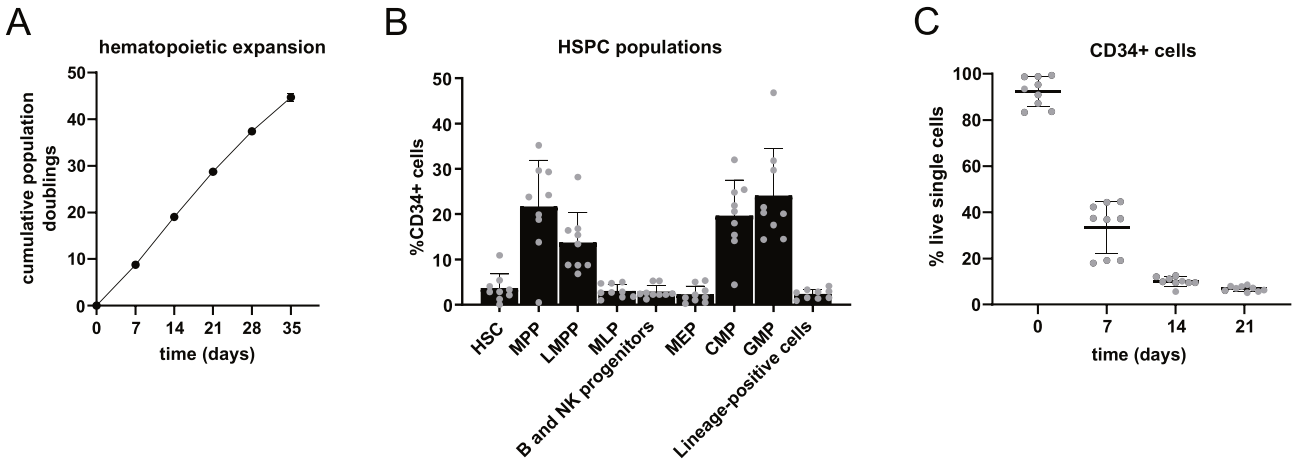

Fig. 1. CB CD34+ HSPC dynamics in B cell differentiation culture conditions. (**A**) Expansion of hematopoietic cells during B cell differentiation depicted as the cumulative population doubling over time. (**B**) Immunophenotypic characterization of CD34+ progenitor populations in freshly isolated CB HSPCs on day 0. (**C**) Fraction of CD34+ cells measured at experimental time points as a percentage of the live cells. Error bars indicate mean ± SD of n = 9 independent biological CB units.

Under B cell differentiation conditions, the HSCs (CD34+CD38-CD90+), MPPs and LMPPs (CD34+CD38-CD90-CD45RA+) (Fig. 2A, first row, 2B) generated CD38- early lymphoid-primed MLP (CD34+CD38-CD45RA+CD10+) population peaks on day 7 (22.98 ± 17.02%) and day 14 (20.78 ± 9.03%). By day 21, the early hematopoietic progenitors were pushed to proliferate towards the CD10+lymphoid primed B/NK progenitor state (74.99 ± 7.65%) (Fig. 2A, third row, 2C), accompanied by a significant reduction in the MEP (CD34+CD38+CD135-CD45RA-), CMP and GMP myeloid progenitor populations (Fig. 2A, fourth row, 2D).

B cell differentiation generates CD38+CD10+ early and CD19+ late committed progenitors in vitro

The CD38+CD10+ CLP state marks the beginning of lymphoid commitment in hematopoiesis[25]. During in vitro B cell differentiation, the CD38+CD10+ population was already established (56.14 ± 15.06%) by day 7 (Fig. 3A, first row, 3B), the majority of which were CD34+ CLPs (29.59 ± 18.20%) (Fig. 3C). The CD10- PreProB (1.24 ± 0.72% of CD45+ live cells on day 21) and CD10+ ProB (1.06 ± 0.006%) populations, identified as the earliest B-committed fetal progenitors[26], were also detectable (Fig. 3A, C, D). They are distinguished from the CLPs by expression of the early pre-B cell receptor (pre-BCR) subunit CD79α. The pre-BCR complex is essential for quality control during differentiation, allowing only cells with a successfully rearranged μH chain to progress further[27]. Notably, the PreProB population was CD45low, similar to early CD34+ hematopoietic progenitors. The remaining CD38+CD10- cells were identified as CD33+CD11b+ expressing monocytes, which were observed to form aggregates in culture if the cell density was too high (data not shown).

The earliest B progenitor to express CD19 was identified as the PreBI cell, which arose in small numbers throughout the differentiation process and peaked on day 35 (1.70 ± 2.19%) (Fig. 3A and C). The CD34-CD19+ PreBII (large) and PreBII (small) cells were distinguished by the expression of CD179α, and these two populations represented the majority of CD19+ cells by day 35 (Fig. 3A, second row, 3E, F). Only a small fraction of cells (0.23 ± 0.05%) expressing IgM were observed on day 35, although it was not attempted to extend the cultures beyond this timepoint. The gating strategy for flow cytometry is shown in the supplementary material (Supplementary Fig. 2).

Since rearrangement of the immunoglobulin heavy chain (*IGH*) locus is the hallmark of developing B cells, rearrangement between D_H and J_H gene segments in early B cell precursors sorted from differentiation cultures was investigated to detect molecular evidence of functional recombinase activity during B cell development as described previously[28]. Evidence of ongoing D_HJ_H rearrangements was detected in fluorescence-activated cell sorting (FACS) sorted CD34+CD10+ and CD34-CD10+ populations across multiple differentiation cultures, with distinct variability between the CBs (Fig. 3G). Taken together, these results demonstrate that the B cell differentiation model system could successfully drive CB CD34+ HSPCs towards functional CD19+ expressing B cells, with immunophenotypically identifiable progenitor populations. The presence of recombined D_HJ_H segments is a hallmark of B lineage commitment, showing successful activity of the recombination machinery during differentiation.

IL-15 supplementation drives CB-derived CD34+ HSPCs to differentiate towards NK cells

IL-15 promotes NK cell development by activating key signaling pathways including JAK-STAT5, PI3K-AKT-mTOR, and RAS-MEK-MAPK, driving NK cell maturation, survival and function[29,30]. Using a modified cytokine cocktail for NK cell specific differentiation (Table 1), significant quantities of hematopoietic cells were generated in the NK cell differentiation system (CPD = 10.66 ± 0.57) (Fig. 4A) across n = 6 independent biological CB replicates. Compared to the B cell differentiation system, the population doublings were lower, however this was attributed to the lower concentrations of SCF and FLT3-L (Table 1), which promote expansion of early hematopoietic progenitors.

As previously mentioned, heterogeneity was found between the CB samples upon immunophenotyping of the HSPC lineages (gated as in Fig. 2A, Supplemental Fig. 1) on day 0, with enrichment in the MPP, CMP and GMP fractions (Fig. 4B). Under NK cell differentiation conditions, there was a significant reduction in CD34+ progenitors from day 0 (88.91 ± 5.1%) to day 21 (5.44 ± 2.35%) (Fig. 4C). The early hematopoietic progenitors (HSCs, MPPs, LMPPs) were lost by day 14 (Fig. 4D). This exhaustion of the early hematopoietic progenitors from the culture system also seems to be a contributing factor to limited cell expansion compared to the B cell differentiation system. There was a skew towards the CD10+ B/NKP cells by 21 days (66.33 ± 8.74%) (Fig. 4E), and a significant reduction in CMP (19.16 ± 4.28% to 2.99 ± 0.43%) and GMP (20.33 ± 4.89% to 3.00 ± 0.95%) myeloid progenitors (Fig. 4F). It was established that the addition of IL-15 to the cytokine cocktail had no detrimental impact on the HSPC populations heading towards the lymphoid lineage.

The key stages of NK cell differentiation from HSCs through the CLP, NKP and iNK stages have been previously described[31]. A flow cytometric strategy (Fig. 5A and B, Supplementary Fig. 3) to identify these populations in the NK cell co-culture system was employed. CLPs were detectable on day 7 (5.27 ± 1.03%) (Fig. 5B, E). NKPs, which are characterized by expression of CD122, were also most abundant at day 7 (3.28 ± 1.11%) (Fig. 5B and E). There were most likely higher percentages of these progenitors prior to day 7, but due to the significant loss of CD34+ populations after day 7 CLPs and NKPs were found only in low numbers after this time point. The iNK cells, found in the fetal liver during early development[32], were detected in significant numbers on day 7 (24.94 ± 6.14%), and day 14 (27.15 ± 9.41%) (Fig. 5C and E). Definitive CD56+ NK cells began to emerge as early as day 14 (0.81 ± 0.76%) in culture and reached a peak at day 35 (28.46 ± 7.01%) (Fig. 5A and E). It was not possible to discern between the dominant CD56bright and the more mature but rarer CD56dim populations due to panel limitations, but analysis of CD16 expression demonstrated the emergence of a more cytotoxic CD56+CD16+ NK cell population by day 35 (30.26 ± 9.22% of CD56+ cells) (Fig. 5D and F). Other NK-specific markers, i.e. KIR2DL1, NKG2D and NKG2A, were detectable on the CD56+ cells starting day 21 (Fig. 5G).

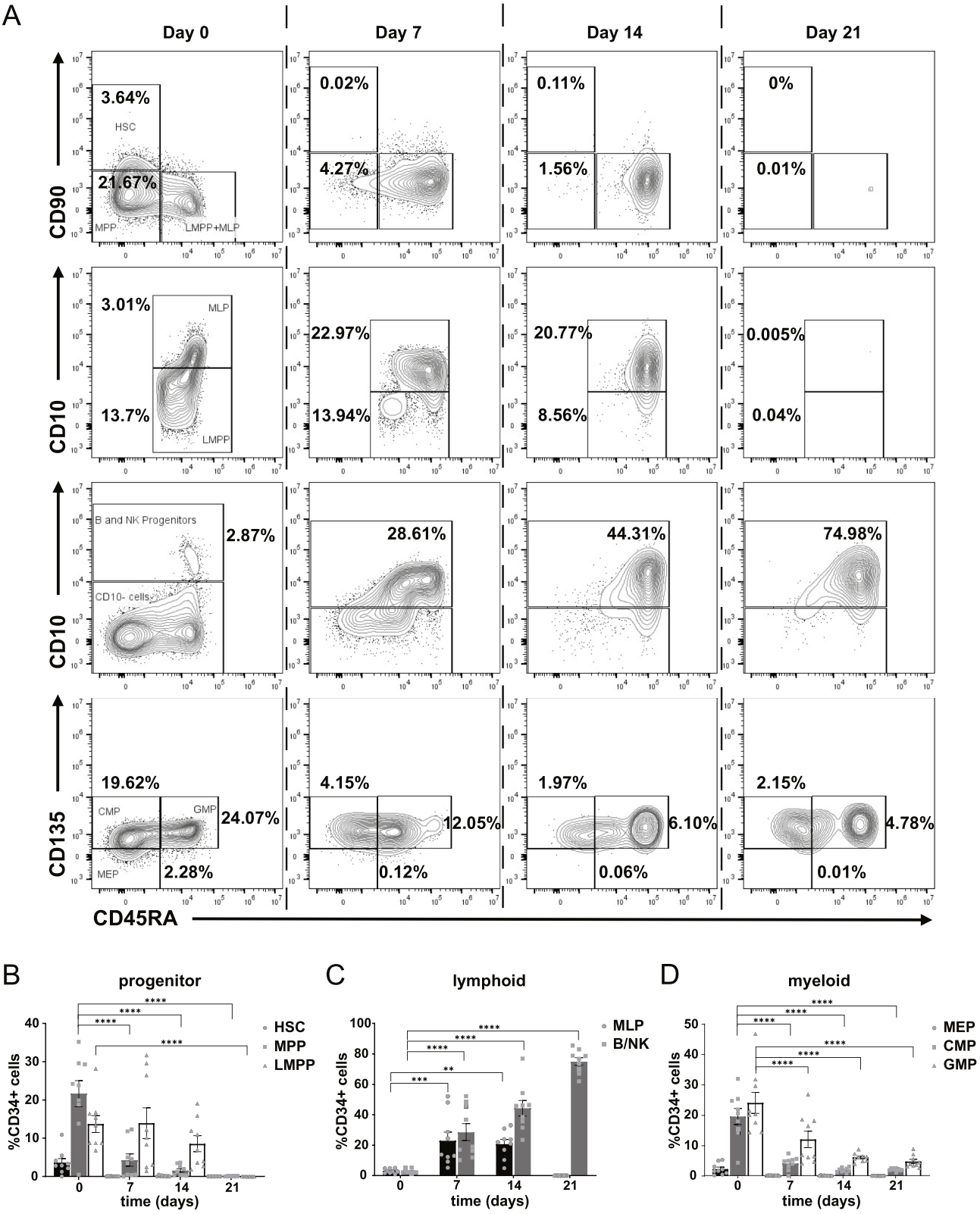

As with the B cell differentiation, the remaining cells in culture were identified as CD33+CD11b+ expressing monocytes, with similar aggregation characteristics at high cell densities (data not shown).

NK cells generated in vitro effectively kill K-562 target cells in co-culture

The cytotoxic potential of differentiated NK cells was evaluated using a standard killing assay[33]. Differentiated NK cells were first isolated on DAPI-CD45+CD56+ by FACS and subsequently co-cultured with the K-562 target cell line. Following co-culture, both NK and target cells were analysed by flow cytometry to assess target cell death, NK cell degranulation, and the expression of surface markers relevant to NK–target cell interactions. NK cell-

◀**Fig. 2**. Development of LIN-CD34+ hematopoietic progenitor cells in B cell culture conditions. (**A**) First row: CD90 expression discriminates between the earliest HSC population and the MPPs in the CD34+CD38- compartment. Second row: CD10 expression distinguishes the CD45RA+ cells into LMPPs and MLPs in the CD34+CD38- compartment. Third row: CD10 expression separates the CD34+CD38+ compartment into the CD10+ B and NK cell progenitors and myeloid progenitors. Fourth Row: The CD10- compartment consists of the MEPs, CMPs and GMPs. Percentages indicated as a proportion of CD34+ cells at each experimental time point. (**B**) Distribution of the earliest hematopoietic progenitors (HSCs, MPPs and LMPPs), (**C**) lymphoid-primed progenitors expressing CD10 (MLPs, B/NK progenitors), and (**D**) myeloid-primed progenitors. Error bars indicate the mean ± SD of n = 9 biological replicates. A two-way ANOVA for multiple comparisons was performed to determine statistical significance (** $p < 0.01$, *** $p < 0.001$, **** $p < 0.0001$).

mediated cytotoxicity resulted in an excess target cell death rate of 55.37 ± 7.77%, while NK cell degranulation increased by 14.24 ± 2.80% (Fig. 6A). The relative mean fluorescence intensity (MFI) of most surface markers remained largely unchanged, apart from PD-L1 (MFI 5.55 ± 2.47) (Fig. 6B). To further quantify cytokine and effector molecule release, supernatants from the co-cultures were subjected to ELISA for IFN-γ and Granzyme B detection. The relative analyte secretion levels of IFN-γ (2.41 ± 1.47) and Granzyme B (1.58 ± 0.22) were found to be modestly elevated (Fig. 6C). These results show that NK cells produced in this co-culture system have active cytotoxic activity and can secrete cytokines upon stimulation.

Discussion

In response to a necessity for a straightforward yet versatile model system that can recapitulate fetal B cell and NK cell development within pre-clinical research settings, the objective was to establish a protocol to generate B and NK cells in sufficient quantities for experimentation. Additionally, we aimed to develop a robust approach to identify and characterize emerging progenitor populations during in vitro culture. Recent single-cell transcriptomic studies demonstrated more complex heterogeneity in human hematopoietic precursors than previously understood, emphasizing the necessity for a more detailed characterization of emerging progenitor populations in in vitro differentiation systems[34,35]. Here, we demonstrate (1) a humanized, serum-free stromal co-culture system enabling scalable production of early/late B cell progenitors from human CB HSPCs, (2) directed differentiation towards CD56+ NK cells via exogenous IL-15 supplementation, and (3) streamlined flow cytometric approaches to track hematopoietic populations developing in vitro.

B cell differentiation systems utilizing co-culture with murine stromal cells[36] have substantially advanced research across multiple disciplines, including developmental biology[37,38] and pediatric leukemia[39]. These stromal feeder layers provide a supportive microenvironment that mimics in vivo conditions, enabling the proliferation, survival and differentiation of B cell progenitors through both direct cell–cell interactions and the secretion of soluble factors such as cytokines[40,41]. Current understanding of hematopoietic progenitor populations is primarily derived from murine-based models[42], despite documented functional disparities between murine and human stromal cells in HSPC maintenance and differentiation[43,44]. It was previously demonstrated that using human BM-MSCs as feeder can produce B lymphocytes from CB CD34+ cells[45]. Although these studies successfully generated CD19+ cells, in many instances, high purities did not translate into fold-expansion numbers necessary for downstream applications. The serum-free formulations allow for greater control over the differentiation process, as well as reproducibility for downstream applications by minimizing interactions with genotoxic/therapeutic compounds, that may adversely react to the presence of serum[46]. In addition, serum-free differentiation systems are more amenable to scale-up for large-scale cell production and regulatory compliance. Maintaining the system within budgetary constraints and at a practical scale for laboratory use remained key considerations in the development of this differentiation model.

As previously noted in the results, CB CD34+ HSPCs are enriched for MPPs and myeloid progenitors. By following the differentiation process immunophenotypically, it was demonstrated that despite inherent biological variability, the differentiation conditions preferentially promoted the expansion of CD10+ progenitors, subsequently generating CD19+ B cell populations. Analysis of stage-specific marker expression confirmed that all phases of B cell development up to the IgM+ stage were recapitulated in this system. The capacity to repeatedly passage earlier progenitors (day 14 and earlier) onto multiple stromal feeder layers demonstrated the robust scalability of the differentiation protocol. It is important to note that permitting uncontrolled expansion of hematopoietic progenitors within a confined culture environment may result in rapid cell death and impaired B lineage cell production, favouring differentiation towards monocytes instead[47]. Feeder cells are essential in most published protocols, with murine stromal lines MS-5 and OP9 providing the microenvironment for lymphoid commitment[48,49]. Human BM-MSCs, however, replicate the hematopoietic niche faithfully by secreting human-specific cytokines (e.g. CXCL12, TGF-β, SCF, FLT3L, IL7) and cell–cell signalling (ICAM-1, VCAM-1, CD166)[50,51]. In the model system described here, co-culture with human BM-MSCs yielded higher proportions of CD38+CD10+ lymphoid progenitors and CD10+CD19+ B cells within 4 weeks compared to previous protocols[48]. The choice of serum-free media also played a role in this.

In contrast, NK cells have been efficiently differentiated in vitro from CB CD34+ cells, with excellent yields obtained from good manufacturing practice compliant protocols[5,9,20]. This is increasingly important for immunotherapy due to the need for large numbers of functional NK cells and the advantages offered by CB as a source[52]. Feeder cell usage diverges significantly, with OP9 and K562 feeder cells for differentiation and expansion achieving high yields of NK cells[53]. Feeder-free methods leveraging cytokine cocktails and Notch-ligand coatings yield lower frequencies of NK cells but avoid contamination risks from foreign cells[54]. A modification to the B cell differentiation system with the addition of IL-15 over five weeks was made. This approach enabled

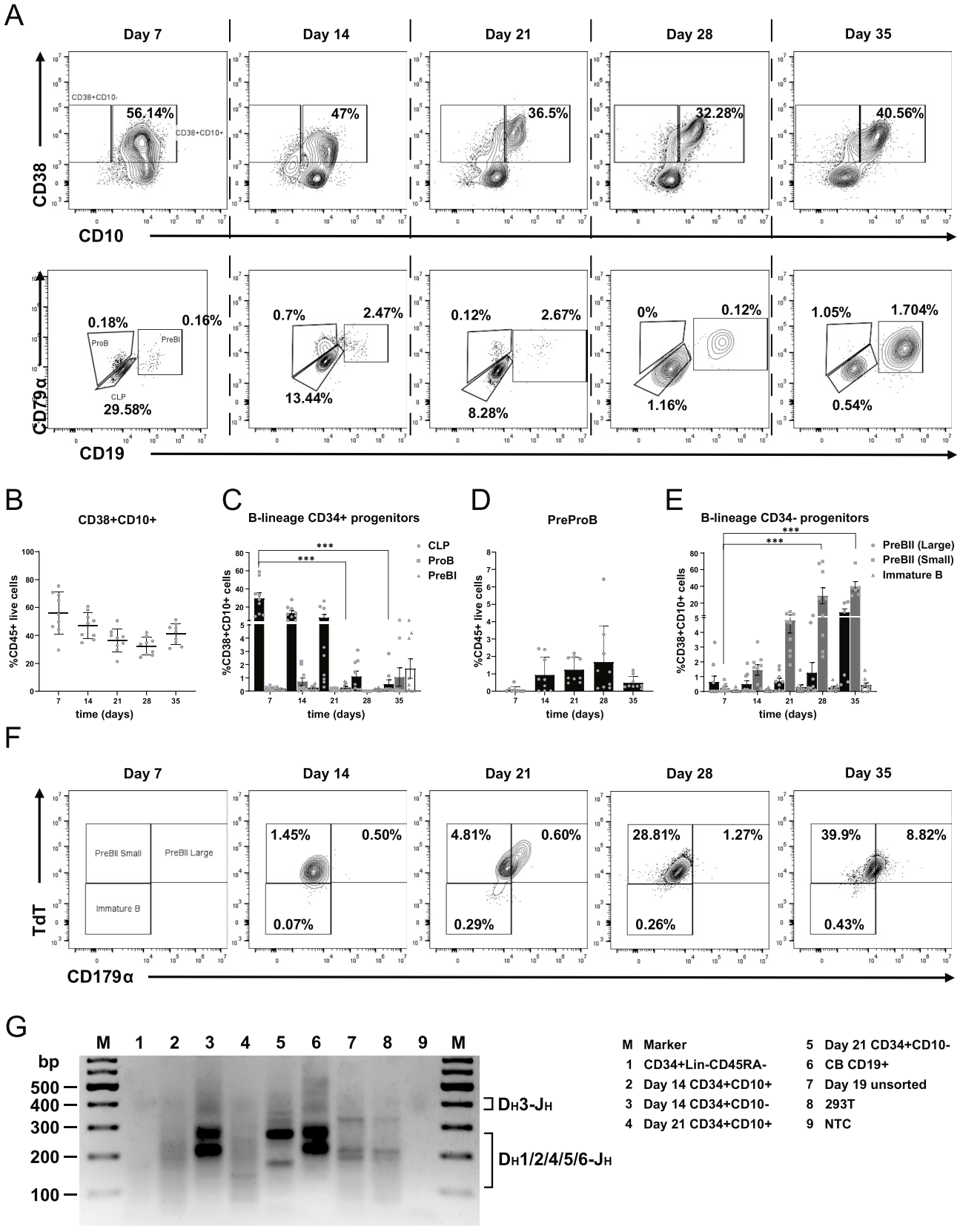

a reduction in the costs associated with establishing a new model system, while still attaining a high overall fold expansion. Importantly, the functional properties of the NK cells were in line with previously described protocols, demonstrating cytotoxic activity towards K-562 target cells as well as NK cell degranulation[18,52]. Further optimization of the media conditions, and the addition of cytokines such as IL-2 are intended to increase the CD56+ yield even further and ameliorate the rapid loss of CD34+ progenitors at the earlier time points[55].

◀**Fig. 3**. Early B lineage committed progenitors arising in co-culture conditions. (**A**) First row: CD38+CD10+ cells include all lineage-committed B progenitors from the CLP to the IgM-expressing immature B cell. Percentages shown are as a proportion of CD45+ live single cells at each experimental time point. Second row: The early B progenitors still express CD34. The CLPs give rise to the ProB cells, which express CD79α and CD179α, and upon gaining CD19 expression become PreBI cells. Percentages shown are as a proportion of CD38+CD10+ cells at each experimental time point. (**B**) CD38+CD10+ cells as a percentage of the CD45+ hematopoietic cells in culture. (**C**) Emergence of CD34+ B progenitors as a percentage of CD38+ CD10+ cells. (**D**) PreProB is the earliest known B-committed progenitor, and resides in the CD38+CD10- compartment, here shown as a percentage of the CD45+ live hematopoietic cells. (**E**) The CD34-CD19+ compartment consists of the PreBII small/large and the Immature B cells. Error bars indicate the mean ± SD of n = 9 biological replicates. A two-way ANOVA for multiple comparisons was performed to determine statistical significance (***$p < 0.001$). (**F**) Emergence of CD34-CD19+ B populations (PreBII(large), PreBII(small) and ImmatureB) over 35 days. Percentages shown are as a proportion of CD38+CD10+ cells at each experimental time point. (**G**) Agarose gel of *IGH* D_HJ_H rearrangements in sorted cells from B cell differentiation experiments (n = 3). Labels for the lanes are shown to the right. Predicted *IGH* rearrangements: $D_H1/2/4/5/6\text{-}J_H$ between 110 and 290 bp; $D_H3\text{-}J_H$ between 390 and 420 bp[28]. Positive control: sorted CB CD34-CD19+ B cells. Negative control: sorted CB CD34+Lin-CD45RA- HSPCs. NTC: no-template control. DNA ladder: GeneRuler 100 bp Plus DNA ladder.

Human recombinant cytokine	Final concentration
B cell differentiation	
Stem cell factor (SCF)	50 ng/mL
Interleukin-7 (IL-7)	25 ng/mL
Fms-related tyrosine kinase 3 ligand (FLT3-L)	50 ng/mL
Interleukin-3 (IL-3, removed from day 7 onwards)	10 ng/mL
NK cell differentiation	
SCF	20 ng/mL
IL-7	20 ng/mL
FLT3-L	10 ng/mL
IL-3 (removed from day 7 onwards)	10 ng/mL
Interleukin-15 (IL-15)	10 ng/mL

Table 1. Cytokine cocktails for B and NK cell differentiation.

The relatively low proportions of NK cell progenitor populations in proportion to CD56+ emergence may be addressed by further immunophenotypic identification, such as CD7+ ProT populations[56].

It must be mentioned here that feeder-free protocols for both B and NK cell differentiation are available, however they require the establishment of two separate culture systems[56,57]. There are also protocols published where antibody-producing plasmablasts were generated from CD34+ HSPCs, albeit using murine stromal cells[58]. With regards to NK cell differentiation, Corredera et al. achieved 80–95% NK cell purity from CB-HSPCs using a two-step differentiation with Notch ligand-coated vessels but included FCS throughout[59]. Lupo et al. reported 17–32% purity from induced pluripotent stem cells in a feeder- and serum-free system on Matrigel-coated vessels, a xenogeneic substrate. Purity increased to 70% only after NK cell expansion with human AB serum[60]. Future studies aim to validate our model system for use with induced pluripotent stem cell-derived HSPCs, to explore developmental susceptibility of progenitor cells to oncogene-induced processes[61].

In conclusion, the results presented above suggest that the serum-free, co-culture system presented here provides a developmentally relevant setting for the examination of B and NK cell progenitors with a minimal set of requirements. This system requires a low input of CB HSPCs, factors in donor variability and consistently generates robust yields of hematopoietic progenitors that can be characterized by flow cytometry. This system will be used to analyse the lymphoid differentiation characteristics of different populations of progenitors arising from preleukemic translocations in early progenitors[62,63], and to identify defects in B and NK cell lymphopoiesis induced by exogenous environmental toxins[64]. It is also intended to further characterize sorted populations at bulk and single-cell RNA transcriptomic level.

Methods

Materials and consumables

A complete list of materials is provided in the supplement (Supplemental Table 1).

Human CB and BM-MSC collection

CB units used for this research were obtained from donations collected by the José Carreras Cord Blood Bank Düsseldorf with the informed consent from the mothers. Collection and use of these samples in experiments was approved by the local ethics commission (Medizinische Fakultät Ethikkommission, UKD-HHU, approval votes 2975, 5279, 2020-1144, 2020-9221). All CB units had a gestational age ≥ 36 weeks. The primary human BM-MSC

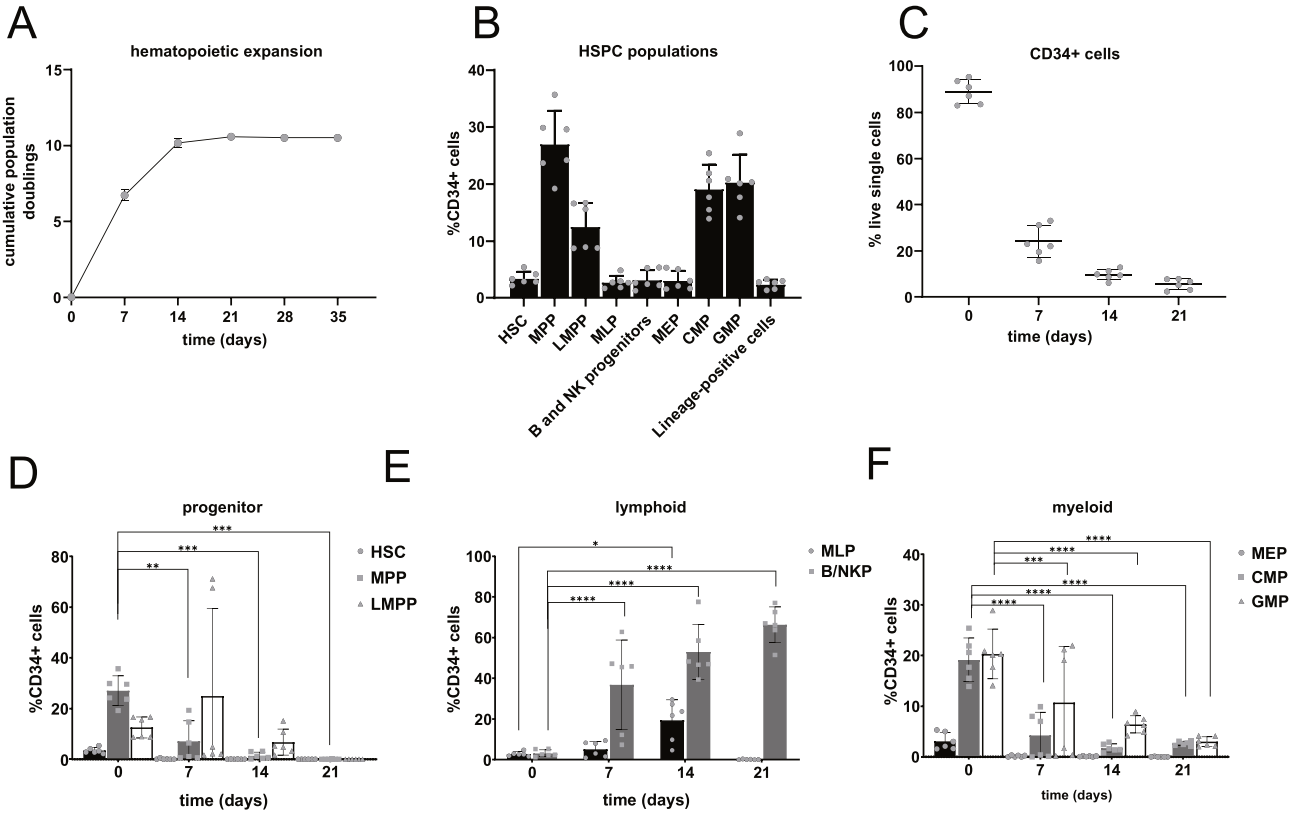

Fig. 4. Development of CD34+ hematopoietic progenitor cells in NK cell culture conditions. (**A**) Expansion of hematopoietic cells during NK cell differentiation depicted as the cumulative population doubling over time. (**B**) Immunophenotypic characterization of CD34+ progenitor populations found in freshly isolated CB HSPCs. (**C**) Fraction of CD34+ cells measured at experimental time points as a percentage of the live cells. (**D**) Distribution of the earliest hematopoietic progenitors (HSCs, MPPs and LMPPs), (**E**) lymphoid-primed progenitors expressing CD10 (MLPa, B/NK progenitors), and (**F**) myeloid-primed progenitors (MEPs, CMPs and GMPs). Error bars indicate the mean ± SD of n = 6 biological replicates. A two-way ANOVA for multiple comparisons was performed to determine statistical significance (*$p < 0.05$, **$p < 0.01$, ***$p < 0.001$, ****$p < 0.0001$).

line KM 9/14 was generated with donor consent and with ethical approval for use in experiments obtained before the initiation of this study (Medizinische Fakultät Ethikkommission, UKD-HHU, approval votes 5884R, 3484). All methods on human tissue samples were carried out in accordance with relevant guidelines and regulations.

CD34+ HSPC isolation and cell counting

Pre-enrichment of the mononuclear cell (MNC) fraction was performed by 1.077 g/cm^3 BioColl® (lymphocytes, Bio-Sell) density gradient centrifugation. CD34+ HSPCs were isolated from the MNC fraction using the CD34 MicroBead Kit, UltraPure, Human (Miltenyi Biotech) according to the manufacturer's instructions. Purity of the CD34+ HSPCs was determined by CD34/CD45/7AAD flow cytometry using a CytoFLEX S Flow Cytometer (Beckman Coulter) according to ISHAGE standards[65]. CD34+ purity of > 80% was considered sufficient for use in experiments, and calculations for cell seeding were adjusted for CD34+ purity.

Cell counting and proliferation assessment

Total nucleated cell counts (TNCs) of CB and MNCs were determined using an automated hematology analyzer (Cell-Dyn Ruby, Abbott Diagnostics). Manual cell counting of CD34+ HSPCs and differentiated cells in suspension was performed using Trypan Blue dye (Sigma-Aldrich) in a 1:1 ratio with an improved Neubauer chamber slide (NanoEnTek). Cumulative population doublings (CPD) were calculated using the formula: $PD = [\log(n_1/n_0)]/\log 2$; $CPD = \sum PD$; n_1 = number of cells counted, n_0 = number of plated cells.

BM-MSC feeder cell culture

The primary human BM-MSC line KM-9/14, derived in-house from a healthy adult donor as previously described[66], was used at passages P7-P9 without irradiation. Cells were thawed 48 h before each experiment and plated at 2×10^5 cells per well in 6-well tissue-culture treated plates in Dulbecco's modified Eagle medium, 1 g/L glucose (DMEM, Gibco) supplemented with 30% fetal bovine serum (FBS, Gibco) and 1% penicillin/streptomycin (Lonza) to achieve 70% confluency on day 0.

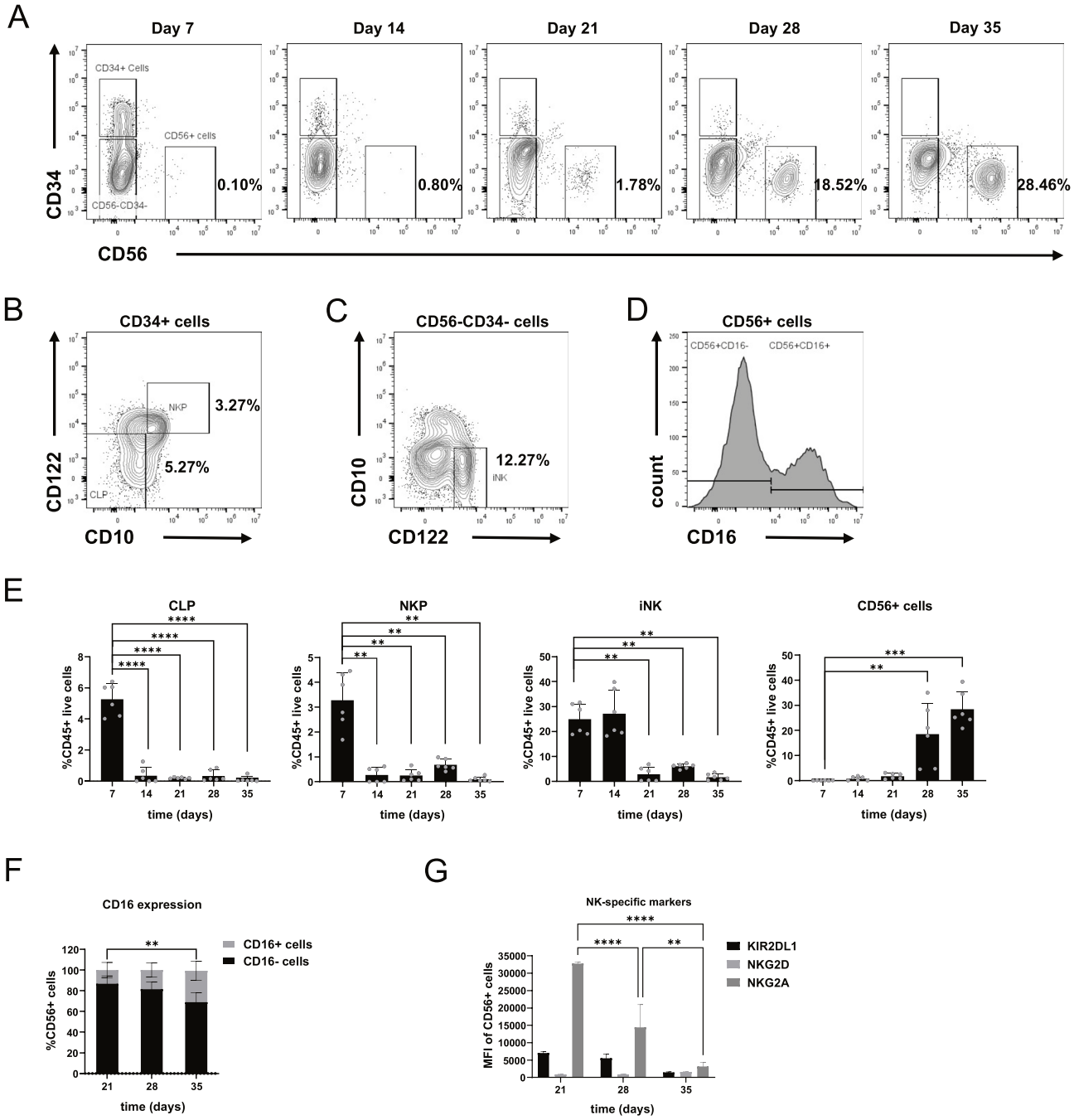

Fig. 5. Differentiation of CB HSPCs towards CD56+ NK cells in co-culture system. (**A**) Representative flow cytometry plots demonstrating initial loss of CD34+ HSPCs and emergence of CD56+ NK cells over 35 days. Plots are gated on the CD45+ live populations, and sub-gated to identify (**B**) CLP, NKP and **(C)** iNK progenitor populations. Percentages inside plots indicate the mean proportions as a fraction of CD45+ live cells. (**D**) Histogram of CD16 expressing CD56+ cells. (**E**) Emergence of various NK cell populations over the course of 35 days. (**F**) CD56+ cells begin expressing CD16 from day 21 onwards. (**G**) Mean fluorescence intensities (MFI) of NK-specific markers expressed on CD56+ cells. Error bars indicate mean ± SD of n = 6 independent biological CB samples. A two-way ANOVA for multiple comparisons was performed to determine statistical significance (**$p < 0.01$, ***$p < 0.001$, ****$p < 0.0001$).

In vitro differentiation cultures

Freshly isolated CB CD34+ HSPCs (1×10^4 to 1×10^5 cells per well) were co-cultured on BM-MSC feeder layers at 70% confluency in 2 mL StemSpan™ SFEM II media (STEMCELL Technologies) supplemented with recombinant human cytokines on day 0. Cytokine cocktails for B and NK cell differentiation are listed in Table 1. On day 7, 2 mL additional media was added, and half-media changes were carried out hereafter every 3–4 days until day

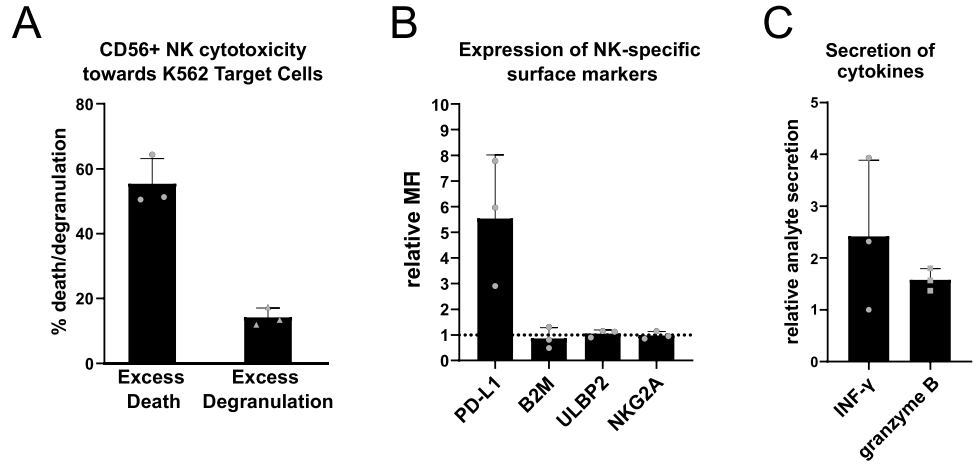

Fig. 6. Functionality of day 35 CD56+ sorted NK cells. (**A**) Cytotoxicity of differentiated NK cells sorted on CD56 represented by percent of excess K-562 target cell death (left) and excess NK cell degranulation marked by CD107a expression (right). (**B**) Relative MFI of major surface markers involved in NK cell killing activity. The dotted line represents the reference baseline for control cells (**C**) Secretion of analytes into the supernatant of co-cultured CD56+ NK cells and K562 target cells relative to NK cell monoculture. Error bars indicate the mean ± SD of n = 3 independent biological CB samples.

35. To prevent excessive cell death due to HSPC expansion, suspension cell concentrations were maintained below 2×10^6/mL by replating onto fresh feeder cells as required.

Flow cytometric characterization

To characterize the CB CD34+ HSPCs (Supplemental Fig. 1) from various time points during differentiation, the following cell surface marker combinations were used[67]:

Hematopoietic stem cells (HSCs): LIN-CD34+CD38-CD90+CD45RA-
Multipotent progenitors (MPP): LIN-CD34+CD38-CD90-CD45RA-
Lympho-myeloid primed progenitors (LMPP): LIN-CD34+CD38-CD90-CD45RA+CD10-
Multi-lymphoid progenitors (MLP): LIN-CD34+CD38-CD90-CD45RA+CD10+
Pre-B lymphocyte/ NK progenitors (pre-B/NK): LIN-CD34+CD38+CD45RA±CD10+
Common myeloid progenitors (CMP): LIN-CD34+CD38+CD10-CD45RA-CD135+
Megakaryocyte-erythroid progenitors: LIN-CD34+CD38+CD10-CD45RA-CD135-
Granulocyte-monocyte progenitors (GMP): LIN-CD34+CD38+CD10-CD45RA+CD135+

Population percentages are expressed as a fraction of the CD34+ live cells, as the BM-MSC feeder cells do not express this marker.

For characterization of the B lineage progenitors arising in vitro during differentiation (Supplemental Fig. 2), the following surface marker and intracellular marker combinations were applied[68].

Common lymphoid progenitors (CLP): CD45+CD34+CD38+CD10+CD127±CD19-cyCD79α-cyTDT-cyCD179α-
PreProB: CD45+CD34+CD38+CD10-CD127+CD19-cyCD79α+cyTDT-cyCD179α-
ProB: CD45+CD34+CD38+CD10+CD127+CD19-cyCD79α+cyTDT+cyCD179α-
PreBI: CD45+CD34+CD38+CD10+CD127+CD19+cyCD79α+cyTDT+cyCD179α+
PreBII (Large): CD45+CD34-CD38+CD10+CD127-CD19+cyCD79α+cyTDT+cyCD179α+
PreBII (Small): CD45+CD34-CD38+CD10+CD127-CD19+cyCD79α+cyTDT+cyCD179α-
Immature B: CD45+CD34-CD38+CD10+CD127-CD19+cyCD79α+cyTDT-cyCD179α-IgM+

Cytoplasmic antibody staining was performed with the BD IntraSure™ kit (BD Biosciences) as per the manufacturer's protocol. Population percentages are given as a fraction of the CD38+CD10+ cells, unless stated otherwise.

For characterization of the NK cell progenitors arising in vitro during differentiation (Supplemental Fig. 3), the following surface marker combinations were used:

NK progenitors (NKP): CD34+CD38+CD45+CD10+CD122+
immature NK cells (iNK): CD34-CD38+CD45+CD10-CD122+NKG2D±
CD56bright NK cells:CD34-CD38+CD45+CD10-CD122+CD56brightCD16±NKG2D+NKG2A+KIR-
CD56dim NK cells: CD34-CD38+CD45+CD10-CD122+CD56dimCD16+NKG2D+NKG2A±KIR±

Population percentages are given as a fraction of the CD45+ live single cells, unless stated otherwise.

Dead cells were excluded using 7AAD (Beckman Coulter) or FVS660/FVS780 (BD Biosciences) depending on the panel (see Supplementary material). Data was acquired on a CytoFLEX S instrument and analyzed using FlowJo™ v10.8 Software (FlowJo LLC). All antibody stainings were performed according to the manufacturer's protocols in FACS buffer (DPBS + 2% FBS) at 1:100 (surface staining) and 1:50 (cytoplasmic staining) dilutions. Gating was determined using fluorescence minus one (FMO) and unstained controls at each time point and

a combination of compensation beads (BD Biosciences) and CB MNCs were used to establish single-stained controls.

Multiplex PCR for detection of DJ rearrangement
CD34+CD10+ and CD34-CD10+ cells sorted on day 14 and day 21, and unsorted cells on day 19 of B cell differentiation were preserved as dry pellets at − 80 °C. Pellets were thawed on ice for DNA extraction using the QIAamp DNA Blood Mini Kit (Qiagen). 100 ng of DNA was taken for PCR reactions with Absolute QPCR SYBR Mix (ThermoFisher Scientific) according to the manufacturer's protocol. Primer sequences described in literature[28] were obtained (Eurofins Genomics) with the following sequences. D_H1: GGCGGAATGTGTGCA GGC; D_H2: GCACTGGGCTCAGAGTCCTCT; D_H3: GTGGCCCTGGGAATATAAAA; D_H4: AGATCCCCA GGACGCAGCA; D_H5: CAGGGGGACACTGTGCATGT; D_H6: TGACCCCAGCAAGGGAAGG; D_H7: CACA GGCCCCCTACCAGC; J_H consensus: CTTACCTGAGGAGACGGTGACC. Primers were combined into two reactions—one with D_H1-6 and J_H consensus primers and another with D_H7 and J_H consensus primers. Samples were run with the following program: an initial hold at 95 °C for 15 min, followed by 50 cycles of 30 s at 95 °C, 30 s at 65 °C and 45 s at 72 °C, ending with a single step at 72 °C for 10 min. A final cycle of 15 s at 95 °C, 20 s at 60 °C and 15 s at 95 °C was followed by a hold at 4 °C. PCR products were run on a 2% agarose gel (Carl Roth) in tris–borate-EDTA buffer. Gels were imaged using an INTAS Gel Documentation System (INTAS Science Imaging GmbH, Germany, software GelDoc System v.0.2.22) under UV transillumination (excitation wavelength 312 nm, shutter time 740 ms). Brightness and contrast were uniformly adjusted using the BioVoxxel Figure Tools *5D Contrast Optimizer* and color inversion was performed using the *LUT Channels Tool* (Fiji/ImageJ https://doi.org/10.5281/zenodo.7268127). Only linear adjustments were applied, and the full uncropped, unedited gel image is provided in the Supplementary material (Supplementary Fig. 4).

Flow cytometry-based NK cell cytotoxicity and degranulation assays
CD56+ NK cells were isolated by flow cytometric sorting on day 35 of differentiation and incubated overnight under standard cell culture conditions (37 °C, 5% CO_2, humidified atmosphere) in 96-well U-bottom plates. Each well contained 100 µL of NK cell activation medium, consisting of RPMI GlutaMAX supplemented with 10% human AB serum, 30,000 U/mL interleukin-2 (IL-2), and 0.3 ng/mL interleukin-15 (IL-15). NK cell numbers seeded for downstream assays varied depending on the yield obtained from cell sorting. For CB1, 75,000 NK cells were seeded per well (n = 3); for CB2, 60,000 NK cells were seeded per well (n = 2); and for CB3, 50,000 NK cells were seeded per well (n = 2). Monocultures at the corresponding cell densities were included as controls for each CB. On the following day, K-562 target cells (DSMZ, ACC 10) were labeled with 0.17 µM CellTrace™ carboxyfluorescein succinimidyl ester (CFSE, Invitrogen) dye and the staining reaction was quenched by addition of RPMI GlutaMAX supplemented with 10% FBS according to the manufacturer's instructions. CFSE-labeled K-562 cells were added to the NK cells at an effector-to-target (E: T) ratio of 1:1. Cells were co-cultured for 4 h at 37 °C and 5% CO_2. Following incubation, supernatants were collected and stored at -80 °C until further analysis by enzyme-linked immunosorbent assay (ELISA). The cells in the pellet were stained for flow cytometric analysis (1:300 antibody dilution, Supplementary Table 1). Target cell killing was quantified as follows: Excess target cell death = % of dead target cells in co-culture—% of dead target cells in monoculture. Degranulation of NK cells during co-culture was measured by cell surface expression of CD107a[69]. NK cell degranulation was calculated as follows: Excess degranulation of NK cells = % of CD107a+ NK cells in co-culture—% of CD107a+ NK cells in monoculture.

Enzyme-linked immunosorbent assay (ELISA)
Secretion of interferon-gamma (INF-γ) as well as Granzyme B by NK cells was analyzed using the human INF-γ and Granzyme B DuoSet ELISA kit (R&D Systems) following the manufacturer's instructions. For granzyme B detection, supernatants harvested during NK cell cytotoxicity assays were diluted 1:2. Relative analyte secretion was determined as follows: Relative analyte secretion = $C_{analyte}$ in co-culture/$C_{analyte}$ in monoculture.

Statistical analysis and figure creation
Row means standard deviation and two-way ANOVA with Dunnet's multiple comparison tests for flow cytometric data, and statistical analysis of NK cell cytotoxicity assays and ELISAs were performed using GraphPad Prism v8.0.2 (GraphPad Software). Image creation and figure assembly was performed on Inkscape v1.4 (The Inkscape Project).

Data availability
The data underlying this article are available in the article and in the supplementary material.

Received: 18 July 2025; Accepted: 26 November 2025
Published online: 18 December 2025

References
1. Doulatov, S., Notta, F., Laurenti, E. & Dick, J. E. Hematopoiesis: A human perspective. *Cell Stem Cell* **10**(2), 120–136 (2012).
2. Notta, F. et al. Isolation of single human hematopoietic stem cells capable of long-term multilineage engraftment. *Science. (1979)* **333**(6039), 218–221 (2011).
3. Yadav, P., Vats, R., Bano, A. & Bhardwaj, R. Hematopoietic stem cells culture, expansion and differentiation: An insight into variable and available media. *Int. J. Stem Cells.* **13**(3), 326. https://doi.org/10.15283/IJSC19157 (2020).
4. Ballen, K. K., Gluckman, E. & Broxmeyer, H. E. Umbilical cord blood transplantation: The first 25 years and beyond. *Blood* **122**(4), 491–498. https://doi.org/10.1182/BLOOD-2013-02-453175 (2013).

5. Shi, P. A., Luchsinger, L. L., Greally, J. M. & Delaney, C. S. Umbilical cord blood: An undervalued and underutilized resource in allogeneic hematopoietic Stem cell transplant and novel cell therapy applications. *Curr. Opin. Hematol.* **29**(6), 317. https://doi.org/10.1097/MOH.0000000000000732 (2022).
6. Mayani, H., Wagner, J. E. & Broxmeyer, H. E. Cord blood research, banking, and transplantation: achievements, challenges, and perspectives. *Bone Marrow Transplant* **55**(1), 48–61. https://doi.org/10.1038/s41409-019-0546-9 (2019).
7. Wang, J. & Metheny, L. Umbilical cord blood derived cellular therapy: advances in clinical development. *Front. Oncol.* **13**, 1167266. https://doi.org/10.3389/FONC.2023.1167266 (2023).
8. Pegram, H. J. et al. IL-12-secreting CD19-targeted cord blood-derived T cells for the immunotherapy of B-cell acute lymphoblastic leukemia. *Leukemia* **29**(2), 415–422. https://doi.org/10.1038/leu.2014.215 (2014).
9. Liu, W. L. et al. Off-the-shelf allogeneic natural killer cells for the treatment of COVID-19. *Mol. Ther. Methods Clin. Dev.* https://doi.org/10.1016/j.omtm.2024.101361 (2024).
10. McCullar, V. et al. Mouse fetal and embryonic liver cells differentiate human umbilical cord blood progenitors into CD56-negative natural killer cell precursors in the absence of interleukin-15. *Exp. Hematol.* **36**(5), 598–608. https://doi.org/10.1016/j.exphem.2008.01.001 (2008).
11. Richardson, S. E., Ghazanfari, R., Chhetri, J., Enver, T. & Böiers, C. In vitro differentiation of human pluripotent stem cells into the B lineage using OP9-MS5 co-culture. *STAR Protoc.* https://doi.org/10.1016/J.XPRO.2021.100420 (2021).
12. Hao, Q. L. et al. Identification of a novel, human multilymphoid progenitor in cord blood. *Blood* **97**(12), 3683–3690. https://doi.org/10.1182/BLOOD.V97.12.3683 (2001).
13. Nishihara, M. et al. A combination of stem cell factor and granulocyte colony-stimulating factor enhances the growth of human progenitor B cells supported by murine stromal cell line MS-5. *Eur. J. Immunol.* **28**, 855–864 (1998).
14. O'Byrne, S. et al. Discovery of a CD10-negative B-progenitor in human fetal life identifies unique ontogeny-related developmental programs. *Blood* **134**(13), 1059–1071. https://doi.org/10.1182/BLOOD.2019001289 (2019).
15. Ichii, M. et al. Regulation of human B lymphopoiesis by the transforming growth factor-β superfamily in a newly established coculture system using human mesenchymal stem cells as a supportive microenvironment. *Exp Hematol.* **36**(5), 587–597. https://doi.org/10.1016/j.exphem.2007.12.013 (2008).
16. Corcione, A. et al. Human mesenchymal stem cells modulate B-cell functions. *Blood* **107**(1), 367–372. https://doi.org/10.1182/BLOOD-2005-07-2657 (2006).
17. Gothot, A. et al. Prolonged ex vivo culture of human bone marrow mesenchymal stem cells influences their supportive activity toward NOD/SCID-repopulating cells and committed progenitor cells of B lymphoid and myeloid lineages. *Haematologica* **95**, 47–56. https://doi.org/10.3324/haematol.2009.008524 (2010).
18. Spanholtz, J., Preijers, F., Tordoir, M., Trilsbeek, C. & Paardekooper, J. clinical-grade generation of active NK cells from cord blood hematopoietic progenitor cells for immunotherapy using a closed-system culture process. *PLoS ONE* **6**(6), 20740. https://doi.org/10.1371/journal.pone.0020740 (2011).
19. Liu, W. L. et al. Off-the-shelf allogeneic natural killer cells for the treatment of COVID-19. *Mol. Ther. Methods Clin. Dev.* https://doi.org/10.1016/j.omtm.2024.101361 (2024).
20. Chandrasekaran, D. et al. Generation of CAR-NK cells using a notch-mediated cell expansion and differentiation platform. *Blood* **136**(Supplement 1), 42–42. https://doi.org/10.1182/BLOOD-2020-142813 (2020).
21. Zhao, X. et al. NK cell development in a human stem cell niche: KIR expression occurs independently of the presence of HLA class I ligands. *Blood Adv.* **2**(19), 2452. https://doi.org/10.1182/BLOODADVANCES.2018019059 (2018).
22. Yap, C. et al. Variability in CD34+ cell counts in umbilical cord blood: Implications for cord blood transplants. *Gynecol. Obstet. Invest.* **50**(4), 258–259. https://doi.org/10.1159/000010327 (2000).
23. Jones, M., Cunningham, A., Frank, N. & Sethi, D. The monoculture of cord-blood-derived CD34+ cells by an automated, membrane-based dynamic perfusion system with a novel cytokine cocktail. *Stem Cell Rep.* **17**(12), 2585. https://doi.org/10.1016/J.STEMCR.2022.10.006 (2022).
24. Kogler, G. & Liedtke, S. Biology of umbilical cord blood cells. In *Hematopoietic Stem Cell Transplantation and Cellular Therapies for Autoimmune Diseases*. Published online January 1, 92–101 (2021).
25. Ichii, M. et al. The density of CD10 corresponds to commitment and progression in the human B lymphoid lineage. *PLoS ONE* **5**(9), e12954. https://doi.org/10.1371/JOURNAL.PONE.0012954 (2010).
26. O'Byrne, S. et al. Discovery of a CD10-negative B-progenitor in human fetal life identifies unique ontogeny-related developmental programs. *Blood* **134**(13), 1059–1071. https://doi.org/10.1182/BLOOD.2019001289 (2019).
27. Bankovich, A. J. et al. Structural insight into pre-B cell receptor function. *Science. (1979)* **316**(5822), 291–294. https://doi.org/10.1126/SCIENCE.1139412 (2007).
28. van Dongen, J. J. M. et al. Design and standardization of PCR primers and protocols for detection of clonal immunoglobulin and T-cell receptor gene recombinations in suspect lymphoproliferations: Report of the BIOMED-2 concerted action BMH4-CT98-3936. *Leukemia* **17**(12), 2257–2317. https://doi.org/10.1038/SJ.LEU.2403202;KWRD (2003).
29. Wang, X. & Zhao, X. Y. Transcription factors associated with IL-15 cytokine signaling during NK cell development. *Front. Immunol.* **12**, 610789. https://doi.org/10.3389/FIMMU.2021.610789/XML/NLM (2021).
30. Huntington, N. D. et al. IL-15 trans-presentation promotes human NK cell development and differentiation in vivo. *J. Exp. Med.* **206**(1), 25–34. https://doi.org/10.1084/JEM.20082013 (2009).
31. Luevano, M., Madrigal, A. & Saudemont, A. Generation of natural killer cells from hematopoietic stem cells in vitro for immunotherapy. *Cell Mol. Immunol.* **9**(4), 310. https://doi.org/10.1038/CMI.2012.17 (2012).
32. Huntington, N. D., Vosshenrich, C. A. J. & Di Santo, J. P. Developmental pathways that generate natural-killer-cell diversity in mice and humans. *Nat. Rev. Immunol.* **7**(9), 703–714. https://doi.org/10.1038/nri2154 (2007).
33. Kandarian, F., Sunga, G. M., Arango-Saenz, D. & Rossetti, M. A flow cytometry-based cytotoxicity assay for the assessment of human NK cell activity. *J. Vis. Exp.* **2017**(126), 56191. https://doi.org/10.3791/56191 (2017).
34. Sommarin, M. N. E. et al. Single-cell multiomics of human fetal hematopoiesis define a developmental-specific population and a fetal signature. *Blood Adv.* **7**(18), 5325–5340. https://doi.org/10.1182/BLOODADVANCES.2023009808 (2023).
35. Popescu, D. M. et al. Decoding human fetal liver haematopoiesis. *Nature* **574**(7778), 365. https://doi.org/10.1038/S41586-019-1652-Y (2019).
36. Nojima, T. et al. In-vitro derived germinal centre B cells differentially generate memory B or plasma cells in vivo. *Nat. Commun.* **2**(1), 1–11. https://doi.org/10.1038/ncomms1475 (2011).
37. Dubois, F. et al. Toward a better definition of hematopoietic progenitors suitable for B cell differentiation. *PLoS ONE* **15**(12), e0243769. https://doi.org/10.1371/JOURNAL.PONE.0243769 (2020).
38. Calvo, J., BenYoucef, A., Baijer, J., Rouyez, M. C. & Pflumio, F. Assessment of human multi-potent hematopoietic stem/progenitor cell potential using a single in vitro screening system. *PLoS ONE* **7**(11), e50495. https://doi.org/10.1371/JOURNAL.PONE.0050495 (2012).
39. Böiers, C. et al. A human IPS model implicates embryonic B-myeloid fate restriction as developmental susceptibility to B acute lymphoblastic leukemia-associated ETV6-RUNX1. *Dev. Cell.* **44**(3), 362. https://doi.org/10.1016/J.DEVCEL.2017.12.005 (2018).
40. Carsetti, R. The development of B cells in the bone marrow is controlled by the balance between cell-autonomous mechanisms and signals from the microenvironment. *J. Exp. Med.* **191**(1), 5. https://doi.org/10.1084/JEM.191.1.5 (2000).
41. Dorshkind, K. & Landreth, K. S. Regulation of B cell differentiation by bone marrow stromal cells. *Stem Cells.* **10**(1), 12–17. https://doi.org/10.1002/STEM.5530100104 (1992).

42. Schmitt, C. E., Lizama, C. O. & Zovein, A. C. From transplantation to transgenics: Mouse models of developmental hematopoiesis. *Exp. Hematol.* **42**(8), 707–716. https://doi.org/10.1016/J.EXPHEM.2014.06.008 (2014).
43. Reichert, D. et al. Phenotypic, morphological and adhesive differences of human hematopoietic progenitor cells cultured on murine versus human mesenchymal stromal cells. *Sci. Rep.* **5**(1), 1–14 (2015).
44. Komic, H. et al. Continuous map of early hematopoietic stem cell differentiation across human lifetime. *Nat. Commun.* **16**(1), 1–17. https://doi.org/10.1038/s41467-025-57096-y (2025).
45. Ichii, M. et al. Regulation of human B lymphopoiesis by the transforming growth factor-β superfamily in a newly established coculture system using human mesenchymal stem cells as a supportive microenvironment. *Exp Hematol.* **36**(5), 587–597. https://doi.org/10.1016/j.exphem.2007.12.013 (2008).
46. Pilili, J. P. et al. Testing genotoxicity and cytotoxicity strategies for the evaluation of commercial radiosterilized fetal calf sera. *Biologicals* **38**(1), 135–143. https://doi.org/10.1016/j.biologicals.2009.08.014 (2010).
47. Mahadik, B., Hannon, B. & Harley, B. A. C. A computational model of feedback-mediated hematopoietic stem cell differentiation in vitro. *PLoS ONE* **14**(3), e0212502. https://doi.org/10.1371/JOURNAL.PONE.0212502 (2019).
48. Dubois, F. et al. Toward a better definition of hematopoietic progenitors suitable for B cell differentiation. *PLoS ONE* **15**(12), e0243769. https://doi.org/10.1371/JOURNAL.PONE.0243769 (2020).
49. Hirose, Y. et al. B-cell precursors differentiated from cord blood CD34+ cells are more immature than those derived from granulocyte colony-stimulating factor-mobilized peripheral blood CD34+ cells. *Immunology* **104**(4), 410. https://doi.org/10.1046/J.1365-2567.2001.01336.X (2001).
50. Ichii, M., Oritani, K. & Kanakura, Y. Early B lymphocyte development: Similarities and differences in human and mouse. *World J. Stem Cells* **6**(4), 421–431. https://doi.org/10.4252/WJSC.V6.I4.421 (2014).
51. Bonnaure, G., Gervais-St-Amour, C. & Néron, S. Bone marrow mesenchymal stem cells enhance the differentiation of human switched memory B lymphocytes into plasma cells in serum-free medium. *J. Immunol. Res.* **2016**, 7801781. https://doi.org/10.1155/2016/7801781 (2016).
52. Luevano, M. et al. Frozen cord blood hematopoietic stem cells differentiate into higher numbers of functional natural killer cells in vitro than mobilized hematopoietic stem cells or Freshly Isolated cord blood hematopoietic stem cells. *PLoS ONE* **9**(1), e87086. https://doi.org/10.1371/JOURNAL.PONE.0087086 (2014).
53. Wen, W. et al. Enhancing cord blood stem cell-derived NK cell growth and differentiation through hyperosmosis. *Stem Cell. Res. Ther.* **14**(1), 295. https://doi.org/10.1186/S13287-023-03461-X (2023).
54. Martin Corredera, M. et al. Feeder-cell-free system for ex vivo production of natural killer cells from cord blood hematopoietic stem and progenitor cells. *Front. Immunol.* **16**, 1531736. https://doi.org/10.3389/FIMMU.2025.1531736/PDF (2025).
55. Wang, K. S., Ritz, J. & Frank, D. A. IL-2 induces STAT4 activation in primary NK cells and NK cell lines, but not in T cells. *J. Immunol.* **162**(1), 299–304. https://doi.org/10.4049/JIMMUNOL.162.1.299 (1999).
56. Martin Corredera, M. et al. Feeder-cell-free system for ex vivo production of natural killer cells from cord blood hematopoietic stem and progenitor cells. *Front. Immunol.* **16**, 1531736. https://doi.org/10.3389/FIMMU.2025.1531736/XML/NLM (2025).
57. Kraus, H. et al. A feeder-free differentiation system identifies autonomously proliferating B cell precursors in human bone marrow. *J. Immunol.* **192**(3), 1044–1054. https://doi.org/10.4049/JIMMUNOL.1301815 (2014).
58. Luo, X. M. et al. Engineering human hematopoietic stem/progenitor cells to produce a broadly neutralizing anti-HIV antibody after in vitro maturation to human B lymphocytes. *Blood* **113**(7), 1422–1431. https://doi.org/10.1182/BLOOD-2008-09-177139 (2009).
59. Martin Corredera, M. et al. Feeder-cell-free system for ex vivo production of natural killer cells from cord blood hematopoietic stem and progenitor cells. *Front. Immunol.* **16**, 1531736. https://doi.org/10.3389/FIMMU.2025.1531736 (2025).
60. Lupo, K. B., Moon, J. I., Chambers, A. M. & Matosevic, S. Differentiation of natural killer cells from induced pluripotent stem cells under defined, serum- and feeder-free conditions. *Cytotherapy.* **23**(10), 939–952. https://doi.org/10.1016/j.jcyt.2021.05.001 (2021).
61. Jepsen, V. H. et al. H1–0 is a specific mediator of the repressive ETV6::RUNX1 transcriptional landscape in preleukemia and B cell acute lymphoblastic leukemia. *Hemasphere.* **9**(4), e70116. https://doi.org/10.1002/HEM3.70116 (2025).
62. Bhave, R. et al. Abstract 24 development of an in vitro B-cell differentiation model for the characterization of the origin and causation of ETV6::RUNX1+ preleukemic cells. *Stem Cells Transl. Med.* **12**(Supplement_1), S26–S26. https://doi.org/10.1093/STCLTM/SZAD047.025 (2023).
63. Bhave, R. et al. In-depth characterization of B-lineage populations arising during cord blood CD34+ HSPC differentiation for ETV6::RUNX1 progenitor identification. *Stem Cells Transl. Med.* **13**, S33 (2024).
64. Becker, F., Ouzin, M., Liedtke, S., Raba, K. & Kogler, G. DNA damage response after treatment of cycling and quiescent cord blood hematopoietic stem cells with distinct genotoxic noxae. *Stem Cells.* **42**(2), 158–171. https://doi.org/10.1093/STMCLS/SXAD085 (2024).
65. Sutherland, D. R., Anderson, L., Keeney, M., Nayar, R. & Chin-Yee, I. The ISHAGE guidelines for CD34+ cell determination by flow cytometry. *J. Hematother. Stem Cell Res.* **5**(3), 213–226. https://doi.org/10.1089/SCD.1.1996.5.213 (1996).
66. Ouzin, M., Wesselborg, S., Fritz, G. & Kogler, G. Evaluation of genotoxic effects of N-methyl-N-nitroso-urea and etoposide on the differentiation potential of MSCs from umbilical cord blood and bone marrow. *Cells* **13**(24), 2134. https://doi.org/10.3390/CELLS13242134/S1 (2024).
67. Pellin, D. et al. A comprehensive single cell transcriptional landscape of human hematopoietic progenitors. *Nat. Commun.* **10**(1), 2395. https://doi.org/10.1038/S41467-019-10291-0 (2019).
68. Kraus, H. et al. A feeder-free differentiation system identifies autonomously proliferating B cell precursors in human bone marrow. *J. Immunol.* **192**(3), 1044–1054. https://doi.org/10.4049/JIMMUNOL.1301815 (2014).
69. Alter, G., Malenfant, J. M. & Altfeld, M. CD107a as a functional marker for the identification of natural killer cell activity. *J. Immunol. Methods.* **294**(1–2), 15–22. https://doi.org/10.1016/J.JIM.2004.08.008 (2004).

Acknowledgements

The authors would like to thank Janine Korn, Almuth Düppers and Dr. Stefanie Liedtke at the Institute for Transplantation Diagnostics and Cell Therapeutics (Heinrich Heine University, Medical Faculty, Düsseldorf, Germany) for their assistance and expertise in the handling and processing of cord bloods. We would also like to thank the José Carreras Cord Blood Bank, Düsseldorf, for providing infrastructure and access to primary cord blood materials.

Author contributions

R.B.: Conceptualization, investigation, data curation, validation, methodology, formal analysis, visualization, writing—original draft. C.J.K.: Investigation, formal analysis, methodology, validation, writing—review and editing. N.R.: Investigation, formal analysis, validation, resources. E.V.: Investigation, formal analysis, validation, resources. V.H.J.: Methodology, visualization, resources, writing—review and editing. K.R.: Investigation, methodology, writing—review and editing. A.A.P: Funding acquisition, supervision, writing—review and editing. U.F.: Funding acquisition, supervision, conceptualization, writing—review and editing, resources. G.K.: Funding

acquisition, supervision, conceptualization, writing—review and editing, resources.

Funding
Open Access funding enabled and organized by Projekt DEAL. A.A.P., U.F., and G.K. acknowledge support from the Deutsche José Carreras Leukämie-Stiftung (DJCLS 18R/2021). A.A.P. and U.F. also acknowledge support from the Deutsche José Carreras Leukämie-Stiftung (DJCLS 16R/2025). A.A.P. and U.F. are supported by the German Childhood Cancer Foundation (A2023/31). A.A.P., U.F., and G.K. acknowledge support from the German Federal Office for Radiation Protection (Bundesamt für Strahlenschutz, BfS, 3622S32231). AAP is supported by the DZIF (TTU 07-711). A.A.P., U.F., and G.K. acknowledge support from the German Ministry for Research, Technology and Space (Bundesministerium für Forschung, Technologie und Raumfahrt, BMFTR; grant no. 01KD2410A, EDI-4-ALL). U.F. is supported by the Deutsche Forschungsgemeinschaft (DFG, Projektnummer 495318549) and the Deutsche Krebshilfe (DKH; Priority Program Cancer Prevention—Graduate School, 70114736).

Declarations

Competing interests
The authors declare no competing interests.

Ethics approval and consent to participate
CB units for research were obtained from donations collected by the José Carreras Cord Blood Bank Düsseldorf with the informed consent of the mothers and ethical approval (Ethic commission votes 2975, 5279, 2020-1144, 2020-9221). All CB units had a gestational age ≥ 36 weeks.

Additional information
Supplementary Information The online version contains supplementary material available at https://doi.org/10.1038/s41598-025-30732-9.

Correspondence and requests for materials should be addressed to R.B.

Reprints and permissions information is available at www.nature.com/reprints.

Publisher's note Springer Nature remains neutral with regard to jurisdictional claims in published maps and institutional affiliations.

Open Access This article is licensed under a Creative Commons Attribution 4.0 International License, which permits use, sharing, adaptation, distribution and reproduction in any medium or format, as long as you give appropriate credit to the original author(s) and the source, provide a link to the Creative Commons licence, and indicate if changes were made. The images or other third party material in this article are included in the article's Creative Commons licence, unless indicated otherwise in a credit line to the material. If material is not included in the article's Creative Commons licence and your intended use is not permitted by statutory regulation or exceeds the permitted use, you will need to obtain permission directly from the copyright holder. To view a copy of this licence, visit http://creativecommons.org/licenses/by/4.0/.

© The Author(s) 2025